Dual-channel connecting-layer-based embedded reflective splitter

CHENHAO GAO, BO WANG*, CHEN FU, JIMIN FANG, KUNHUA WEN, ZIMING MENG, ZHAOGANG NIE, LI CHEN, LIANG LEI, JINYUN ZHOU
School of Physics and Optoelectronic Engineering, Guangdong University of Technology, Guangzhou 510006, China

We design and optimize dual-channel reflection subwavelength grating with good uniformity. Given an incident wavelength of 1550 nm and grating period of 1540 nm, the simplified modal method can be used to obtain the optimized duty cycle and grating groove depth. By using the rigorous coupled-wave analysis, grating parameters are analyzed and calculated. For TE and TM polarization, a good splitting ratio can be exhibited with 48.5%/48.4% and 48.1%/48.1%, respectively. Previous subwavelength gratings worked only at narrow bandwidth. The designed dual-channel connecting-layer-based embedded reflective grating can show the wide bandwidth.

(Received December 8, 2018; accepted August 20, 2019)

Keywords: Beam splitter, Polarization independence, Reflective efficiency

1. Introduction

Polarization-independent grating [1-5] has been widely used in optical design such as beam splitters [6-9] and converters [10,11]. A beam splitter [12-17] can divide the incoming light into two directions with good uniformity, which is widely used in high-precision laser interferometers [18] and holographic optical tweezers [19]. Polarization-independent dual-channel grating is a kind of beam splitting of TE and TM polarizations into the -1st and the 0th orders, and both of them are close to efficiency of 50%. Li *et al.* [20] have designed a two-channel embedded grating with a single grating layer and connecting layer under the Littrow angle.

This design mainly uses modal method [21] and rigorous coupled-wave analysis (RCWA) [22]. The modal method can explain the theoretical illustration of the grating. Through the analysis and interpretation of the diffraction process, the approximate grating depth is given and the optimization time is reduced. The simplified modal method ignores the influence of evanescent mode and grating interface reflection. The optimal solution requires RCWA for numerical calculation, which is the appropriate method to optimize the grating profiles for precise parameters [23,24]. In addition, a covering layer is added, which can reduce Fresnel loss and improve diffraction efficiency, and the embedded grating can keep the grating surface clean.

In this paper, we propose a dual-channel embedded reflection grating. The grating structure involves the grating region to realize diffraction, the connecting layer to obtain wideband property, and Ag slab to reflect the incident wave. We use the modal method to analyze grating parameters roughly. With the RCWA, we get the optimal results of beam splitter. The efficiency of 48.4%/48.5% and 48.1%/48.1% can be obtained in the -1st and the 0th orders for TE and TM polarizations, respectively. Compared with previous results [20], the bandwidth of the grating is wider.

2. Modal analysis and numerical design

The schematic diagram of dual-channel connecting-layer-based embedded reflection grating can be shown in Fig. 1.

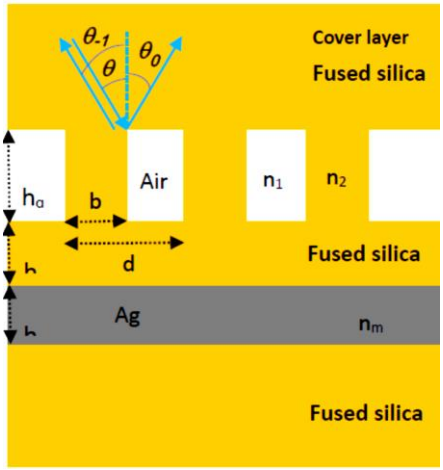

Fig. 1. (Color online) Schematic structure of dual-channel connecting-layer-based embedded reflection grating

As shown in Fig. 1, from the top to the bottom, the grating consists of three parts. The first part is grating covering layer, where its refractive index is n_2 = 1.45. The second part is grating ridge and connecting layer with refractive index of 1.45. The medium of two adjacent grating ridge is air, where the refractive index is n_1=1.0. In the second part, the grating depth and the thickness of connecting layer are h_g and h_c, respectively. The third part is Ag slab, where the refractive index is n_m=0.469-9.32i.

Based on physical mechanism of modal method, the diffraction waves with wavelength of λ can be calculated by the accumulated phase difference for two polarizations. Hence, different phase difference can lead to the efficiency modulation of diffraction orders. The reflected waves will propagate twice in the grating region when they are diffracted. The following equations can be associated with the phase difference, which is denoted by:

$$\Delta\varphi^{TE} = \frac{4\pi}{\lambda}\left(n_{0eff}^{TE} - n_{1eff}^{TE}\right)h_g = (2m+1)\frac{\pi}{2} \quad (1)$$

$$\Delta\varphi^{TM} = \frac{4\pi}{\lambda}\left(n_{0eff}^{TM} - n_{1eff}^{TM}\right)h_g = (2n+1)\frac{\pi}{2} \quad (2)$$

$$\eta_{-1}^{TE} = sin\left(\frac{\Delta\varphi^{TE}}{2}\right)^2 \quad (3)$$

$$\eta_0{}^{TE} = cos\left(\frac{\Delta\varphi^{TE}}{2}\right)^2 \quad (4)$$

$$\eta_{-1}{}^{TM} = sin\left(\frac{\Delta\varphi^{TM}}{2}\right)^2 \quad (5)$$

$$\eta_0^{TM} = cos\left(\frac{\Delta\varphi^{TM}}{2}\right)^2 \quad (6)$$

The Eqs. (1) to (6) represent the interference effect between the excited modes. The light enters the grating and excites two grating modes. The process is similar to the Mach-Zehnder interferometer, and the two-beam interference theory provides a grating coupling efficiency equation based on the effective refractive index. Eqs.(1) and (2) show the phase difference for two polarizations. From Eqs. (3) to (6), when the phase difference meets the odd-numbered of π/2, the efficiency in the -1st order or the 0th order for TE/TM polarization can reach 50%. As a single-layer grating, the effective refractive indices of TE and TM waves satisfy a proportional relation when they meet the modal interpretation:

$$\frac{\Delta\varphi^{TE}}{\Delta\varphi^{TM}} = \frac{\frac{4\pi}{\lambda}\left(n_{0eff}^{TE} - n_{1eff}^{TE}\right)h_g}{\frac{4\pi}{\lambda}\left(n_{0eff}^{TM} - n_{1eff}^{TM}\right)h_g} = \frac{2m+1}{2n+1}, \quad (7)$$

where m and n are both integers, $n_{veff}{}^{TW}$ is the vth effective mode of TW polarization. Considering the practical etching process and the etching material, m and n are selected to be zeros. In order to make the output efficiency 50/50 and keep good uniformity, the corresponding $\Delta\varphi^{TM}/\Delta\varphi^{TE}$ is 1. For the incident wavelength of 1550 nm, and period of 1540 nm.

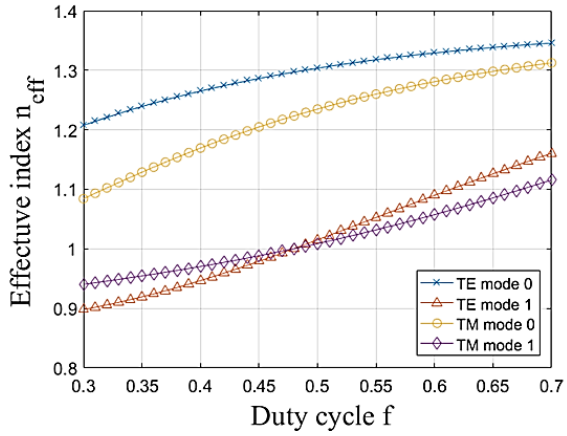

(a)

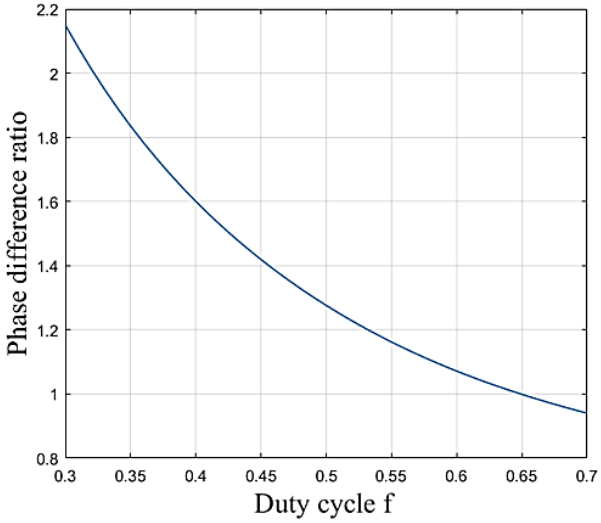

(b)

Fig. 2. (Color online) (a) Effective indices that vary with duty cycle for both polarizations. (b) Ratio of TM polarization phase difference $\Delta\varphi^{TM}$ to TE polarization phase difference $\Delta\varphi^{TE}$ as a function of grating dutycycle

Fig. 2 (a) shows effective index versus duty cycle, which can be chosen to design the grating. Fig. 2 (b) describes the relationship between duty cycle and phase ratio of TM to TE polarization. In the case of duty cycle of 0.65, $\Delta\varphi^{TM}/\Delta\varphi^{TE}$ is 0.9988. The results of each effective index can be calculated with n_{0eff}^{TE} =1.338, n_{1eff}^{TE} =1.126, n_{0eff}^{TM} =1.298, and n_{1eff}^{TM} =1.086. In purpose of obtaining the good efficiencies and good uniformity of

two polarizations, the grating parameters need to be optimized by using RCWA. We first select the duty cycle and period of the grating by modal method, and then optimize the groove depth and the thickness of the connecting layer by the rigorous coupled-wave analysis method. Reflective efficiencies can be calculated for different depths and thicknesses. Dual-channel near 50/50 can be diffracted by choosing proper parameters.

The value of the effective refractive index can be determined by the dispersion equations $F(n_{eff}^2)$ [25], which may be calculated from the intersection of $F(n_{eff}^2)$ and $\cos(\alpha d)=-1$. Fig. 3 shows plot of $F(n_{eff}^2)$ for the grating with the duty cycle of 0.65 and incident wavelength of 1550 nm. The intersections between $F(n_{eff}^2)$ and -1 determine the two grating modes. It can be seen from the figure that the grating excites two modes.

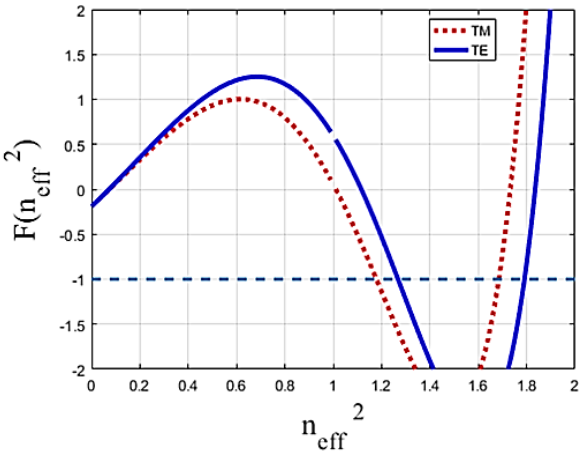

Fig. 3. (Color online) Plot of $F(n_{eff}^2)$ for the grating with the duty cycle of 0.65 and incident wavelength of 1550 nm. The intersections between $F(n_{eff}^2)$ and -1 determine the two grating modes

3. Discussions of tolerance and bandwidths

Fig. 4 shows efficiency versus grating depth layer and thickness of connecting layer with the grating duty cycle of 0.65 and grating period of 1540 nm for working wavelength of 1550 nm. These four figures show reflection efficiencies of TE and TM polarizations in the 0th order and the -1st order. The reflection efficiency of TE polarization in the -1st order and the 0th order can reach 48.5%/48.4% when grating groove depth h_g is 1.10 μm and connecting layer thickness h_c is 0.32 μm. For TM polarization, the diffraction efficiencies in the 0th order and the -1st order are obtained as 48.1%/48.1%, respectively. Therefore, good uniformity can be kept by the proposed grating.

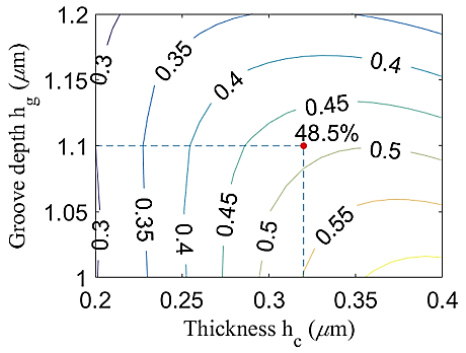

(a)

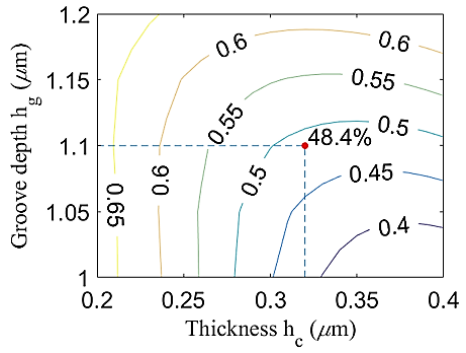

(b)

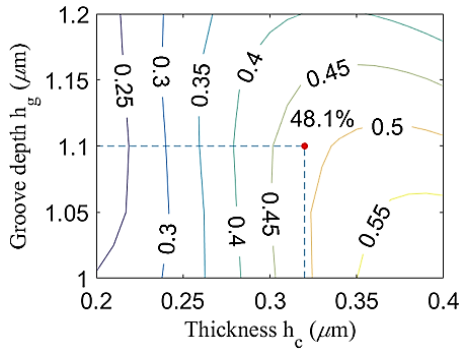

(c)

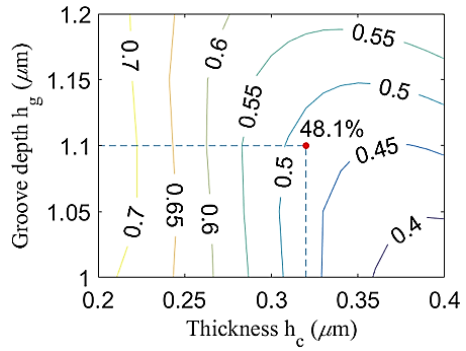

(d)

Fig. 4. (Color online) Reflection efficiency versus grating depth and thickness of the connecting layer: (a) TE polarization in the 0th order, (b) TE polarization in the -1st order, (c) TM polarization in the 0th order, (d) TM polarization in the -1st order.

Considering the etching error in practice, the manufacturing tolerance must be researched. Fig. 5 displays the reflective efficiency versus the grating duty cycle with grating period of 1540 nm at a working wavelength of 1550 nm under the Littrow mounting. As shown in Fig. 5, owing to different duty cycle, the reflection efficiency will change to some extent. In Fig. 5, efficiencies can be greater than 45% in each of the two diffraction orders for TE-polarized light within a duty cycle range of 0.64-0.66. For TM-polarized light, with the duty cycle limit of 0.62-0.67, efficiencies are larger than 45% in both diffraction orders. In industrial manufacturing, a certain industrial tolerance should be considered. For two polarized incident light, the optimal duty cycle of both diffraction orders is 0.64-0.66, which meets the performance requirements.

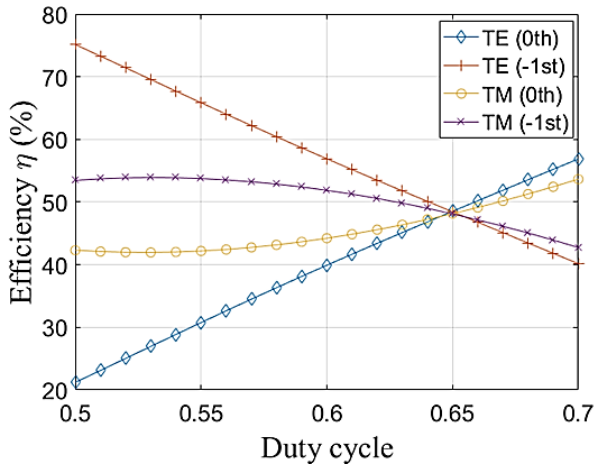

Fig. 5. (Color online)Efficiency versus grating duty cycle for the reflection grating with the optimized parameters

In addition to considering the tolerance of duty cycle, the tolerance of grating period should also be studied. Fig. 6 shows the diffraction efficiency with the different grating period under Littrow mounting. It can be found that good grating efficiency can be obtained for grating period range of 1460-1620 nm by using RCWA. When the grating period is in the range between 1505 nm and 1571 nm, for two polarizations, the diffraction efficiencies of the grating are higher than 45% in both orders. The grating has a relatively wide period tolerance, which is beneficial to the actual industrial production.

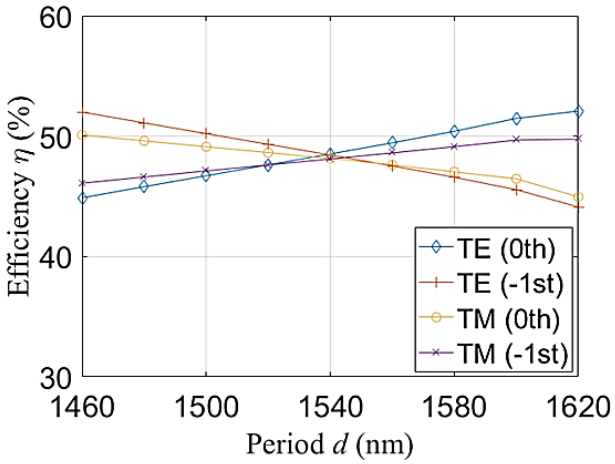

Fig. 6. (Color online) Diffraction efficiency versus grating period with the grating duty cycle of 0.65 at the working wavelength of 1550 nm under Littrow mounting

The incident wavelength of spectral bandwidth can be studied by using the RCWA. Because of the different incident wavelengths, the reflection efficiency of the embedded grating is also different. A good beam splitter should have good incident bandwidth. Figure 7 analyzes the change of grating efficiency in the wavelength range from 1450 nm to 1700 nm.As shown in Fig. 7, TE polarization has the efficiency greater than 45% when the wavelength range is 1513-1612 nm. In addition, for TM polarization light, efficiencies in the both orders are more than 45% when the incident light wavelength is within the range of 1515-1652 nm. For TE and TM polarizations, the grating has a bandwidth of 97 nm (1515-1612 nm).

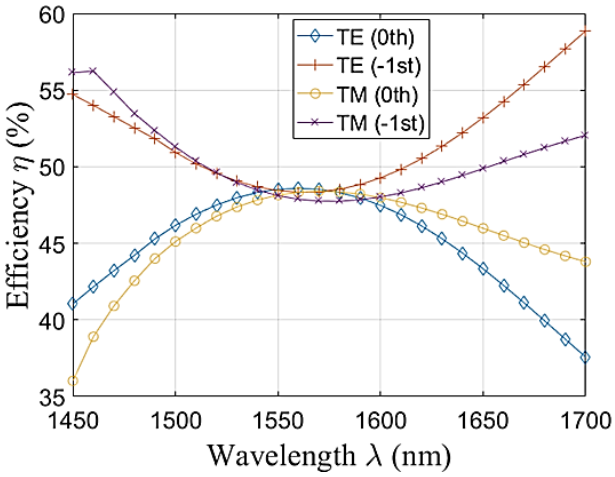

Fig. 7. (Color online) Reflection efficiency versus incident wavelength under Littrow mounting and duty cycle of 0.65.

Similarly, the difference of incident angle will affect the reflection uniformity. Fig. 8 shows the variation of reflection efficiency at the incidence angle from 16° to 24°. The Littrow angle can be represented by $\theta=\sin^{-1}(\lambda/2n_2d)$. With the previous optimized results ofλ=1550 nm, n_2=1.45and d=1540 nm, the angle is 20.33° under Littrow mounting. In Fig. 8, when the incident angle is in the range from 17.9° to 23.4°, for TM polarization in the -1st and the 0th orders, the reflection efficiencies are higher than 45%. Efficiencies of both orders are more than 45% within angle range of 18.2-22.4° for TE polarization. Based on the above optimization calculation, the grating has good operation angular bandwidth of 4.2° (18.2-22.4°) for the incident angle.

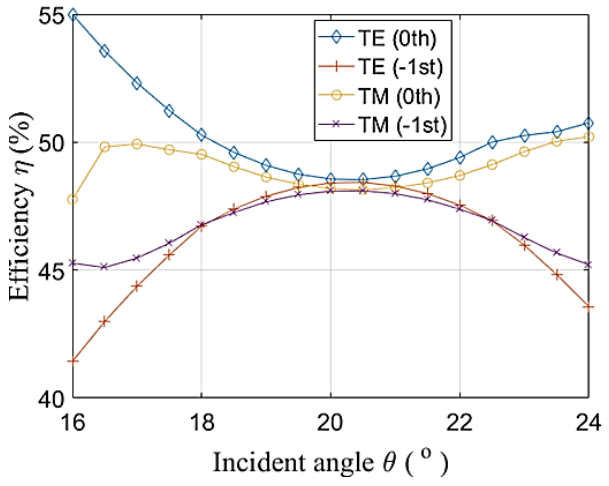

Fig. 8. (Color online) Splitting efficiency of optimized grating versus incident angle at an incident wavelength of 1550 nm.

4. Conclusion

In conclusion, we present a dual-channel connecting-layer-based embedded reflection grating with good uniformity. By the modal method, we get grating duty cycle of 0.65 and grating groove depth of 0.91 μm. RCWA is used to optimize the depth of grating groove and the thickness of connection layer. The optimized grating groove depth and connection layer thickness is 1.10 μm and 0.32 μm at Littrow angle of 20.33° for the incident wavelength of 1550 nm. Diffraction efficiencies of 48.5%/48.4% for TE polarization and 48.1%/48.1% for TM polarization can be obtained. For different incident wavelength and angle, the bandwidth for operation can be exhibited to some extent. For incident wavelength, the bandwidth is 97 nm. And during practical operation, the angular bandwidth is 4.2°. The proposed connecting-layer-based embedded reflection grating can have advantages of polarization-independent property and broad bandwidth.

Acknowledgements

This work is supported by the Foundation for Distinguished Young Talents in Higher Education of Guangdong (KQNCX065), the Science and Technology Planning Projects of Guangdong Province (2016A020223013, 2016B090918124), and the National Natural Science Foundation of China (11604057, 11774071, 61675050, 11774069).

References

[1] D. Wang, Q. Wang, Z. Zhan, IEEE Photon. J. **10**(5), 4501609 (2018).
[2] X. Duan, M. Zhang, Y. Huang, K. Liu, Y. Shang, X. Ren, IEEE Photon. Technol. Lett. **29**(2), 209 017).
[3] L. Nikolaevsky, T. Shchori, D. Malka, IEEE Photon. Technol. Lett. **30**(8), 720 (2018).
[4] H. Cao, J. Wu, J. Yu, J. Ma, Appl. Opt. **57**(4), 900 018).
[5] Z. Zhang, H. Zhu, Q. Cheng, B. Huang, C. Cheng, H. Li, H. Chen, Opt. Commun. **445**, 247 (2019).
[6] J. Cao, J. Wang, G. Yang, Y. Lu, R. Sun, P. Yan, S. Gao, Superlattice Microstruct. **110**, 26 (2017).
[7] L. Xu, Y. Wang, A. Kumar, D. Patel, E. El-Fiky, Z. Xing, R. Li, D. V. Plant, IEEE Photon. Technol. Lett. **30**(4), 403(2018).
[8] H. Yang, K. Ou, G. Cao, X. Shang, Y. Liu, Y. Deng, Opt. Commun. **443**, 104 (2019).
[9] C. Gao, B. Wang, H. Li, K. Wen, Z. Meng, Q. Wang, X. Xing, L. Chen, L. Lei, J. Zhou, Mod. Phys. Lett. B **32**(31), 1850386 (2018).
[10] Y. Cai, Z. Wang, H. Wan, Z. Zhang, L. Zhang, IEEE Photon. Technol. Lett. **31**(14), 1155 (2019).
[11] Y. Hu, S. Wan, J. Shi, X. He, Opt. Commun. **435**, 126 019).
[12] X.-M. Yang, Z.-L. Deng, Mod. Phys. Lett. B **32**(28), 1850335 (2018).
[13] F. Chen, Y. Xu, Mod. Phys. Lett. B **30**(31), 1650376 (2016).
[14] F. Zhang, K. Song, Y. Fan, Sci. Rep. **7**, 41726 (2017).
[15] P. Li, Y. Han, W. Wang, Y. Liu, P. Jin, J. Leng, Sci. Rep. **7**, 44333 (2017).
[16] M. Rohith, C. Sudheesh, R. Rajeev, Mod. Phys. Lett. B **30**(2), 1550269 (2016).
[17] N. Shukla, R. Prakash, Mod. Phys. Lett. B **30**(21), 1650289 (2016).
[18] D.-S. Kim, J.-W. Cho, K. Park, Y.-S. Kim, S.-K. Kim, Curr. Appl. Phys. **17**(8), 1015 (2017).
[19] B. Li, G. Niu, Y. Yi, X.-W. Zhou, X.-D. Liu, L.-X. Sun, C.-Y. Wang, Superlattice Microstruct. **111**, 57 (2017).
[20] H. Li, B. Wang, Sci. Rep. **7**(1), 1309 (2017).
[21] I. C. Botten, M. S. Craig, R. C. Mcphedran, J. L. Adams, J. R. Andrewartha, Opt. Acta. **28**(3),

413 981).
[22] M. G. Moharam, D. A. Pommet, E. B. Grann, T. K. Gaylord, J. Opt. Soc. Am. A **12**(5), 1077 95).
[23] A. Farmani, A. Zarifkar, M. H. Sheikhi, M. Miri, Superlattice Microstruct. **112**, 404(2017).
[24] G. Palumbo, D. Tosi, A. Iadicicco, S. Campopiano, IEEE Photon. J. **10**(3), 7103015 (2018).
[25] H. Pei, B. Wang, W. Zhu, S. Yin, L. Chen, L. Lei, J. Zhou, J. Optoelectron. Adv. M. **19**(11-12), 688 (2017).

*Corresponding author: wangb_wsx@yeah.net